



## Analysis of Extracellular Vesicles Lysing using Surface Acoustic Wave Resonator

Nazihah Zainal<sup>1</sup>, Nur Mas Ayu Jamaludin<sup>2</sup>, Muhamad Ramdzan Buyong<sup>2</sup>, Norazreen Abd Aziz<sup>1,\*</sup>

<sup>1</sup> Faculty of Engineering & Built Environment, Universiti Kebangsaan Malaysia, 43600, Bangi, Selangor, Malaysia

<sup>2</sup> Institute of Microengineering and Nanoelectronics (IMEN), Universiti Kebangsaan Malaysia, 43600, Bangi, Selangor, Malaysia

### ARTICLE INFO

#### Article history:

Received 29 August 2022

Received in revised form 24 Sept. 2020

Accepted 30 September 2022

Available online 30 November 2022

#### Keywords:

Lysing; SAW; AIDT; microfluidic; resonator

### ABSTRACT

The integration of a Y-channel microfluidic system with an annular SAW device developed using MEMS technology has built an efficient platform for mixing and lysing of extracellular vesicles. The travelling SAW used in this study operating at a frequency of 50 MHz is capable of generating surface acoustic waves stream on a liquid sample inside a Y-chamber. At a height of 80µm the PDMS chamber and a liquid sample flow rate of 10µl/min can produce a mixing method that is able to generate gas bubbles that cause the occurrence of microcavities which are the agents of the extracellular vesicle lysing mechanism. This method of rupturing extracellular vesicles through cavitation techniques results in cell rupture through a combination of shear force and pressure changes without destroying proteins and nucleic acids. The Bradford assay is used to observe the increased presence of proteins resulting from the rupture of extracellular vesicles after exposure to acoustic waves. Based on the results, it can be concluded that the most optimal SAW exposure time and power is at 20dBm and 60 seconds. Through this test it can also be observed that a longer exposure period will generate heat which results in the degradation of the proteins that come out of the extracellular vesicles. It can be concluded that the results of this study prove that mechanical method of integrating an annular -SAW device and a Y-channel PDMS microfluidic chamber for micro-mixing, the analysis of biological cells and lysing mechanism can be achieved more effectively compared to conventional methods.

## 1. Introduction

Cell research at the molecular level is essential for disease study, pathogen detection and drug development. Breaking down cells to extract intracellular contents, including DNA, RNA and proteins is a very important first step in cell analysis [1]. Extracellular vesicles, a membrane-derived particles released from cells into circulatory system consists of exosomes and microvesicles of size range 30-100 nm and 100-1000 nm respectively which carry nucleic acids, proteins, lipids and other molecules.

Extracellular vesicles (EVs) are increasingly known for their proven ability as markers to detect disease (biopsies) [2] and also function as a means of communication between cells in the body [3].

\* Corresponding author.

E-mail address: [norazreen@ukm.edu.my](mailto:norazreen@ukm.edu.my)

<https://doi.org/10.37934/araset.28.3.1426>

EVs are heterogeneous vesicles with a phospholipid membrane that are actively secreted by mammalian cells, especially dividing cancer cells and host cells [4,5]. EVs are now the latest target for researchers to study biological tests and possess unique physical and biological characteristics; ranging in size (typically 50–200 nm in diameter) smaller than cells (10–30  $\mu\text{m}$ ) but larger than protein molecules and highly heterogeneous in nature [6]. Various different methods have been developed for the purpose of isolation [7] manipulating [8,9] and breaking EVs. Cell breaking methods in laboratory and industrial scale have been developed and used for years. However, there are many disadvantages such as the use of large samples, the risk of damage to cell vesicles, low purity, and takes a long time, which is difficult to meet the increasing scientific research [10]. The last few years have shown several innovations in microfluidic technology that are able to break down new external cells in one integrated platform and demonstrate the properties of high purity, high throughput and low sample volume consumption [11,12]. The method of creating pores using sound or sonoporation that uses ultrasound interaction with micro bubbles to induce temporary pores on the membrane allows some impermeable molecules to be transferred into the cell [13]. Breaking down of eukaryotic and bacterial cells using the sonication process which is the process of destroying cells or DNA molecules by using high frequency sound waves [14]. The transducer is driven with a sinusoidal source in the 360MHz range. Fragmentation of HL-60 and *Bacillus subtilis* spores was obtained with 80% and 50% respectively using this device.

However, sonication has several limitations and weaknesses such as heat generated, complex mechanisms and expensive fabrication processes. In order to reduce the operation time, the cells need to be treated first with a weak bleach such as digitonin [15] before being exposed to ultrasound. The function of digitonin is to weaken the cell membrane and help in the process of breaking the cell. In addition, Han et al. reported an innovative micro vortex chip by integrating butterfly wings functionalized with lipid nanoprobe into microfluidics to efficiently isolate exosomes from biological fluids [16]. This technique effectively promotes micro-mass transfer of nanoparticles and thus achieves about 70% exosome fragmentation efficiency.

Among the latest approaches for cell disruption methods is the use of surface acoustic waves (SAW) which have greater potential than using conventional ultrasound methods. Previous studies have shown that SAW does not affect the integrity of micro bubbles significantly when the voltage applied to the IDT is smaller than 10V [17]. Islam, Aryasomayajula and Selvaganapathy found that 24MHz SAW was used to induce microwave destruction at desired locations in controlled movements, inducing sonoporation at the single cell level [18]. In 2015, Taller *et al.*, [19] have performed a SAW-on-chip study to detect exosomal RNA to study pancreatic serum. As a result of the research, they managed to achieve a break rate of 38% using this technique.

This work focuses on the integration of the annular-SAW device and Y-microchannel to develop a microfluidic system platform that enables lysing of EVs extracted from colon cancer cells. To achieve this objective, several characterization studies have been conducted including channel height, power supply on SAW devices as well as the duration of acoustic energy exposure that affect the rate of mixing and lysing. The geometry characteristics of the annular-SAW device used in this work has an electrode width of 30  $\mu\text{m}$ , focal length of 500  $\mu\text{m}$  and diameter of 4 mm.

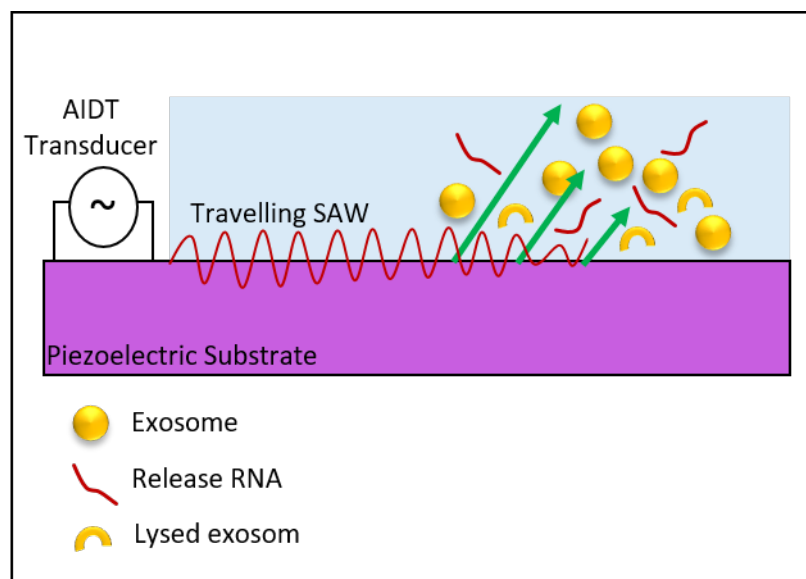


**Fig. 1.** Schematic diagram of the SAW device (side view) and SAW-induced fragmentation to release RNA for detection. The SAW generated at the transducer is refracted into the liquid inducing the movement of the liquid and the electromechanical coupling also generates electric waves on the surface of the substrate [19]

## 2. Experimental Set Up

### 2.1 Lysing Mechanism

Surface acoustic waves (SAW) are used to generate acoustic energy capable of breaking down cells [20]. The mixing technique used in a microfluidic system will produce gas bubbles that cause cavitation to occur. Previous evolution and research were more focused on the fabrication and design of IDT geometries and less focused on applications in fields involving biological samples in particular because biological samples are intricate and difficult to handle. The focused SAW (F-SAW) is capable of generating surface acoustic waves to enable it to transfer and manipulate micro particles as well as liquids in microliter volumes [21]. The vibration of acoustic waves propagating constructively according to the circular IDT shape causes a sample of particles or liquid to concentrate in the central region of the device and due to the resulting force makes it able to break the outer cell vesicles. The F-SAW is capable of performing acoustic mixing when two different fluids are introduced into two inlets using a syringe pump and will mix in a Y-channel microfluidic chamber. The sample and PBS buffer will be introduced into different inlet tubes and will be mixed in the middle of the channel. This concept is applied in the method of dissection of outer cell vesicles. Cell breakdown can be achieved through lysing of outer cell vesicles. Cell disintegration can be achieved through SAW in which Rayleigh waves generated on the surface of the substrate with alternating current are applied through an interdigit electrode transducer [22]. When the SAW wave interacts with the liquid droplets as shown in Figure 1, the wave will produce acoustic pressure in the liquid medium and the electrical components in the wave produce Maxwell electrical pressure between the substrate surface and the liquid. Both these SAW-applied electrical and acoustic pressure interactions have proven useful for focusing and arranging particles and cells [23], producing charged aerosols for mass spectrum permeability [24] and cell breakdown [25].

## 2.2 Device Fabrication

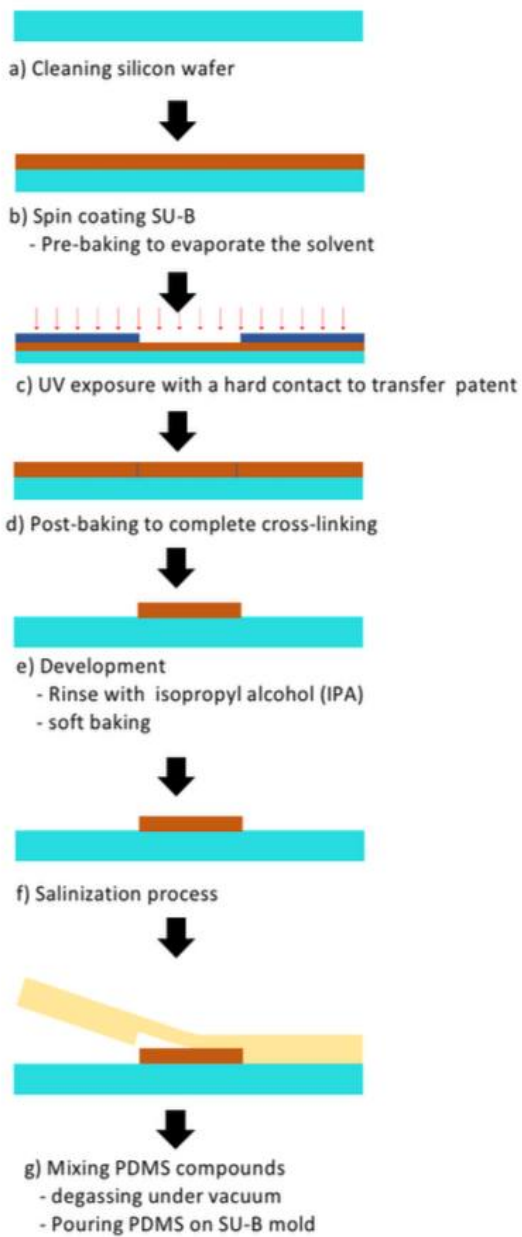
### 2.2.1 Microfabrication of SU-8 mold

To start the fabrication process, the silicon wafer is cleaned in the nanostrip for 10 minutes and then rinsed with deionized water followed by a drying process using nitrogen gas. A SU-8 2075 negative photoresistor is pin-coated on a silicon wafer and then exposed to ultraviolet (UV) light to transfer the mask pattern over the SU-8 layer. At first, 5 ml of SU-8 photoresistor was spin-coated at a speed of 500rpm for 5 seconds and then the spin speed was increased to 3000rpm for 45 seconds to obtain a layer with a thickness of 80 $\mu$ m. The SU-8 coated silicon wafer was kept for 15 minutes to allow the resistor to obtain a uniform thickness. The coated substrate is then "soft baked" on a hot plate at 65°C for 3 minutes and raised to a temperature of 95°C and baked again for 9 minutes. The substrate is then cooled for 10 minutes. After the heat curing process, the substrate is exposed to UV light with a wavelength of 405nm on the black side of the mask for 45 seconds for a 250 $\mu$ m thick photoresist. A post-exposure bake to UV is done immediately so that the film network occurs on a hot plate at 65°C for 2 minutes then raised to 95°C for 7 minutes. Finally, the photoresist layer is developed using the immersion technique in the developer solution (SU-8 Developer) for 7 minutes to form the desired channel structure. The developed wafer is sprayed with isopropyl alcohol (IPA) and dried using filtered and pressurized nitrogen.

### 2.2.2 Fabrication of IDT

The metal lift-off method was selected to fabricate the best annular IDT [26]. Using this method, photoresist layer was lifted to create patterns or structures. This was because any metal thickness below 500 nm may be handled considerably more easily and it is thought to be a non-hazardous operation. The surface acoustic wave (SAW) device's annular electrodes have constant width and pitch thanks to the use of floating-electrode unidirectional transducers (FEUDTs). Per wavelength, FEUDT often uses more than two electrodes. After cleaning the piezoelectric substrate, a coating of HDMS was applied, and then a layer of photoresist AZ 5214E. Prior to the metal deposition of 350 nm thick aurum layer, a 20 nm thick chromium adhesion layer was set down. Using the DC sputtering approach, both thin films were applied to the substrate with power voltage and pressure of up to 200 W and 2 mTorr, respectively. The fabrication process flow for the AIDT device is depicted in Figure 2. For the lift process, the substrate was submerged in an acetone bath with low ultrasonic energy. For convenience of handling and electrical measurement, the substrate was sliced into 2 cm  $\times$  2 cm squares and bonded to a PCB using a SMA connector.

**Microfabrication process steps of SU8 mold, hardened PDMS microchannel integrated microfluidic device**



**Fabrication process flow for AIDT device**

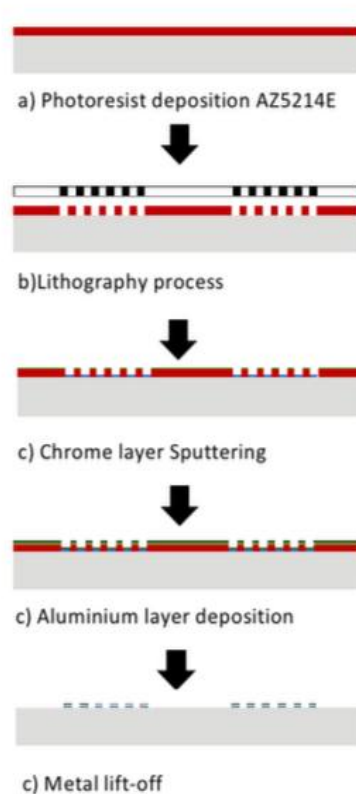


**Fig. 2.** Schematic diagram of fabrication process for SU-8 mold and AIDT

## 2.3 Bradford Assay Characterization

### 2.3.1 Protein concentration measurement using the Bradford Test

Proteins are the most abundant macromolecules in a cell, and also perform important metabolic processes in the cell. In some research applications, the Bradford test is one of the most recommended protein tests compared to other methods such as the Lowry method. First, the Bradford protein test is easier to use because it requires only one reagent and a reaction time of only 5 minutes compared to three reagents and a longer reaction time if using the Lowry method. Second, the Bradford test has a more stable absorption of dye-protein complexes. Moreover, this test is not influenced by other compound substances unlike the Lowry method. Thus, in this study the Bradford test was performed to measure the protein concentration in the outer cell vesicle samples that had been exposed to SAW. The objective was to observe an increase in protein presence before and after exposure was performed. The Bradford protein test was based on the observation that the maximum absorption for Coomassie Brilliant Blue G-250 solution changed from 465 to 595 nm when protein binding occurred. The Standard Curve has a linear relationship between the absorption at  $\lambda = 595$  and the BSA protein concentration ( $\mu\text{g/ml}$ ) needs to be plotted first before the protein concentration of the sample can be found.

**Table 1**  
 Sample manipulation

Sample manipulation	Power (dBm)	Time (sec)	Droplet volume ( $\mu\text{l}$ )				Flow rate ( $\mu\text{l/min}$ )
			FM		Bradford Test		
			Sample	PBS	Sample	PBS	
Without SAW	0	30	0.5	0.5	1.5	1.5	3
		60					5
		90					10
With SAW	5	90	0.5	0.5	1.5	1.5	
	10		0.5	0.5	1.5	1.5	
	15		0.5	0.5	1.5	1.5	
	20		0.5	0.5	1.5	1.5	

## 2.4 Testing Procedure

### 2.4.1 Qualitative and quantitative measure of mixing efficiency by using fluorescent microscope

To evaluate the mixing efficiency, fluorescent images captured with fluorescent microscope (FM) with time averages were taken at different positions on the microfluid channel from where the SAW transducer was placed. FM is used to see the capabilities of a microfluidic parallel flow channel system where it is able to directly visualize the laminar flow of two different fluids; PBS buffer and extracellular vesicle sample as it merges from inlet to main channel where there is parallel flow between PBS and sample. The vesicle sample has been stained first then the cells will be visible under FM. Fluorescence intensity was measured at the top,  $I_u$  and bottom of the SAW transducer,  $I_b$ . Ratios were taken between the top and bottom of the channel to calculate the mixing fraction  $E = I_u / I_b$ ,

which was set as a quantitative measure for mixing efficiency. When the SAW is turned off, the vesicle cells are at the bottom of the duct and are not visible in the upper duct so the fraction of the batter is  $E = l_u/l_l = 0$ . Once mixing and complete distribution of fluorescent vesicle cells across the entire channel is achieved, this yields  $l_u = l_l$  and subsequently  $E = 1$ .

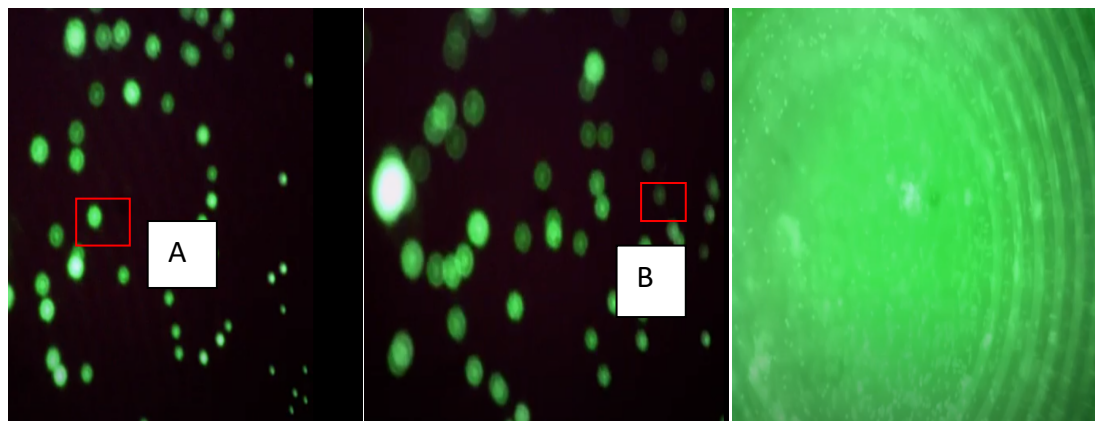


Fig. 3. Distance of particles from point A to point B is measured

Acoustic wave propagates constructively in the shape of a circular IDT will cause the particle or liquid to converge in the central region of the device and able to break the outer cell due to the resulting force. In a previous method [27], it has been proved that F-SAW is capable of performing acoustic mixing in which two different fluids are introduced into two inlets using a syringe pump and will mix in the circular chamber of the Y-microfluidic channel. The microfluidic system consists of a Y-shaped channel with two inlet holes of 1mm diameter at the same angle joined with 4mm diameter circular chamber in the middle. The minimal surface area of the circular channel exposed to the fluid will reduce the friction between the wall surface and the fluid thus reducing the energy consumption to pump the fluid at a given flow rate. Tubes are made with two inlets and one outlet of the same size using a 1mm inner diameter punch and PTFE tube.

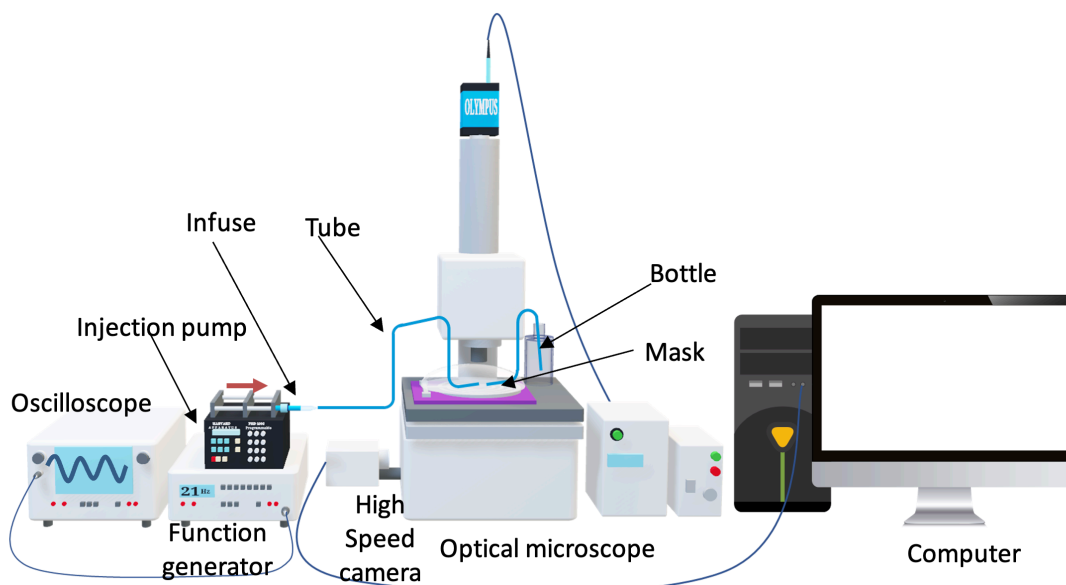
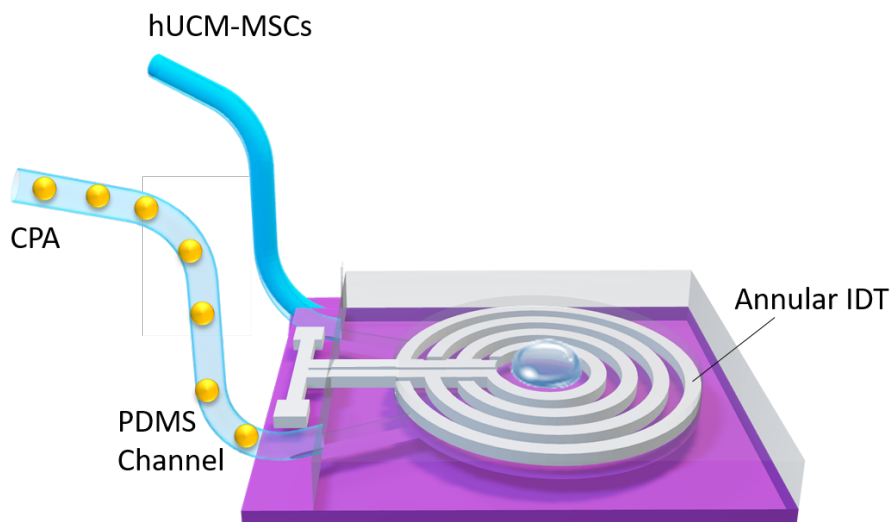


Fig. 4. Schematic diagram of experimental set up



**Fig. 5.** Schematic diagram for device used to study acoustic mixing. 2 PDMS channel inlets were pumped with PBS and sample and mixed in the middle of the chamber integrated with SAW chip

The sample and PBS buffer will be put into the inlet tubes and mixed in the middle of the channel. The concept of mixing is applied in rupturing the membrane of extracellular vesicles. A Y-channel microfluidic system that is fabricated and set to a flow rate with a velocity of  $10\mu\text{l}/\text{min}$  is generated by applying a constant pressure to the inlet. Based on previous mixing experiments,  $10\mu\text{l}/\text{min}$  was chosen as the best optimal flow rate compared to  $3\mu\text{l}/\text{min}$  and  $5\mu\text{l}/\text{min}$  flow rates because the higher the flow velocity, the faster the time for the two liquids to mix.

### 3. Results and Discussion

#### 3.1 Manipulation of Extracellular Vesicles Sample using Fluorescence Microscope

A line graph plotting the SAW -induced mixing efficiency in the channel is shown as in Figure 6. The graph is plotted for the mixing efficiency  $E$  as a function of the distance  $X$  from the transducer downstream towards the channel outlet. For control purposes, no SAW was used to detect the natural laminar flow of the fluid layer until there was diffusion between the two flows. Fluorescent cell vesicles and PBS buffer flow along the channel to approximately  $x = 2\text{mm}$  before a mixture fraction of only  $E = 0.5$  is reached. Once the SAW is generated under the middle channel of the device, the mixing process is accelerated. When the SAW amplitude is gradually increased, the mixing process takes place at a shorter distance from the transducer. At the highest SAW amplitude, complete mixing ( $E = 1$ ) was achieved at a distance of  $X = 4\text{mm}$ , i.e. a factor of 10 less than without mixing. The mixing graph shows a step on the line that could be the result of a vortex vortex leading to a dynamic accumulation of fluorescent cell vesicles in the center of the channel.



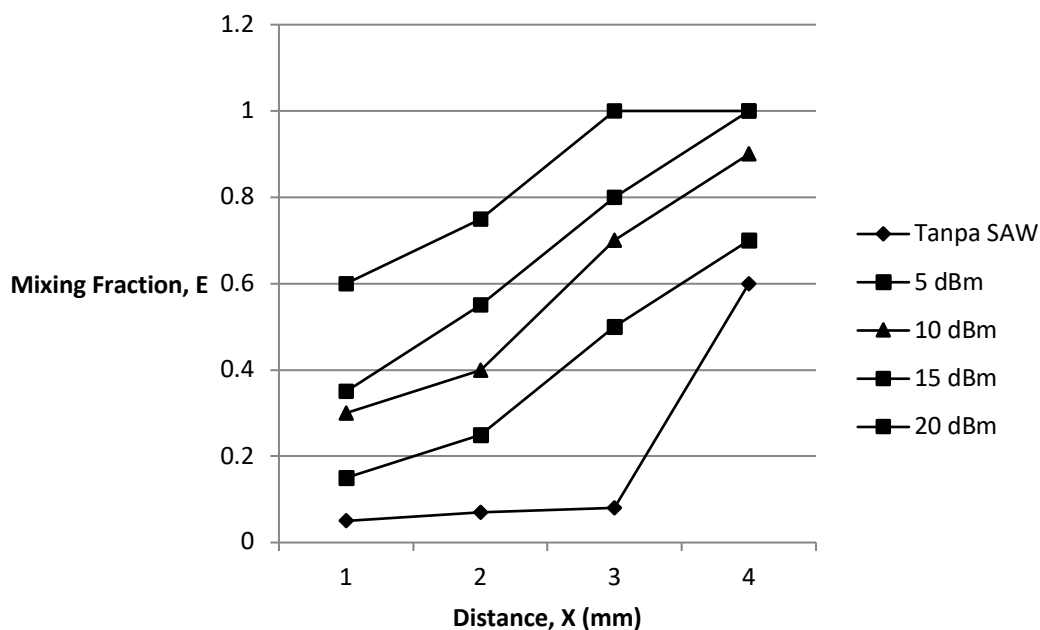


**Fig. 6.** Mixing fraction, E obtained experimentally as a function of distance x from the IDT generating the SAW. Different symbols correspond to different SAW amplitudes

### 3.2 Analysis of Outer Cell Vesicle Breakdown by Measuring Sample Protein Concentration using Bradford Test

After obtaining the absorption readings of the samples exposed to SAW, the Bradford Standard Curve was used to calibrate the total protein concentration in the extracellular vesicle samples. Graphs were made using Microsoft Excel and the results of the sample protein concentrations were extrapolated from the Standard Curve graph or could also be calculated using slopes and y-intercepts from the Standard curve graph. The main objectives of this experiment were to (i) determine the total protein concentration for a sample of outer cell vesicles after exposure to SAW and (ii) study the rate of cleavage of outer cell vesicles when exposed to SAW. The plotted Standard curve is the sample concentration against the sample absorption reading. A line of best fit is obtained from the graph which has the equation  $y = 0.0006x + 0.101$ . In the linear equation, the y-axis represents the absorption reading at a wavelength of 595nm while the x-axis represents the protein concentration of the sample. When comparing the data obtained for the three exposure times, it can be seen that at  $t = 30s$  and  $t = 60s$  the absorption readings are higher if the power is increased. This condition is an indication of an increase in the total protein concentration in the sample after exposure to SAW (refer to graphs A1 and A2). The higher the absorption value, the higher the total protein concentration in the sample. The value of  $R^2$  is 0.964, which is relatively high because it is close to 1 where it gives an indication that the amount of protein in the sample is close to the actual value of the total protein concentration of the sample. Therefore, the standard curves obtained from the data are reliable and can be re-applied to measure protein concentrations for other samples. However, it can be observed that at the exposure time  $t = 90s$ , the total protein concentration in the sample decreases when the power is increased to 15dbm.

Technically, it can be seen through data and graphs that there is an increase and decrease in the total protein concentration of the sample when exposed at such a time, therefore, the second objective studied is the rate of dissection of outer cell vesicles after exposure to SAW waves. An increase in the total protein concentration indicates that something happens to the cell vesicles when

exposed to SAW because these acoustic waves have an acoustic pressure capable of breaking down the cell. Outer cell disintegration is possible and is a realistic phenomenon due to the effects of acoustic radiation forces and dielectric forces acting on small particles [28,29]. When the cell vesicle ruptures, the contents of the cell and plasma in the cell will come out of the vesicle membrane and this condition causes the protein to increase in the sample. Fragmentation of outer cell vesicles can be seen in the results of TEM performed previously. However, acoustic stress will generate heat if exposed for too long and this will cause the proteins coming out of the outer cell vesicles to undergo degradation or destruction and cause the total protein concentration in the cell to decrease.

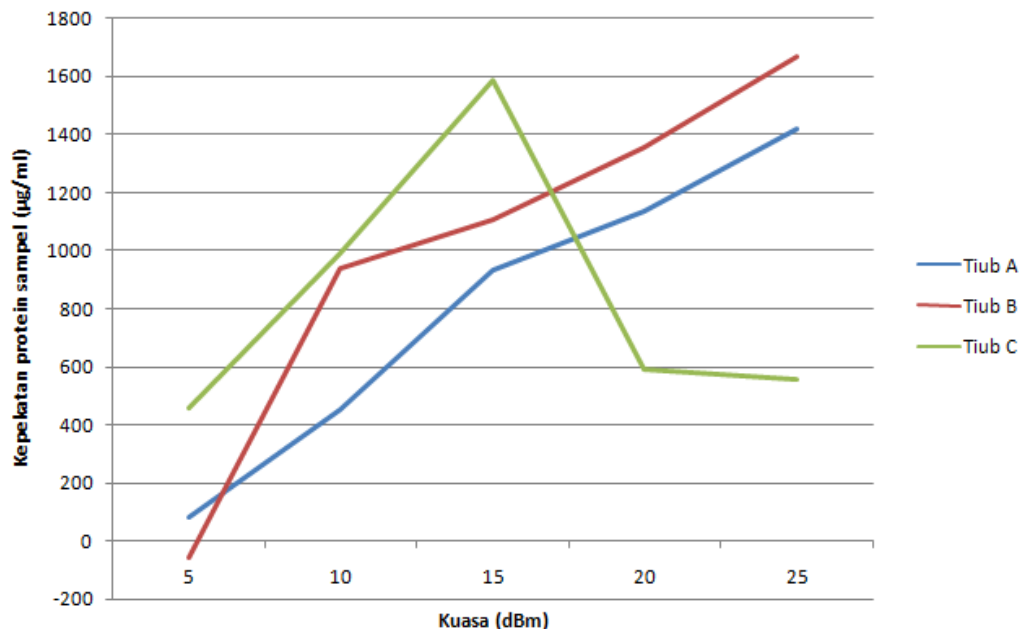


Fig. 7. Comparison graph of protein concentration of tube samples A, B and C when subjected to different power and exposure time

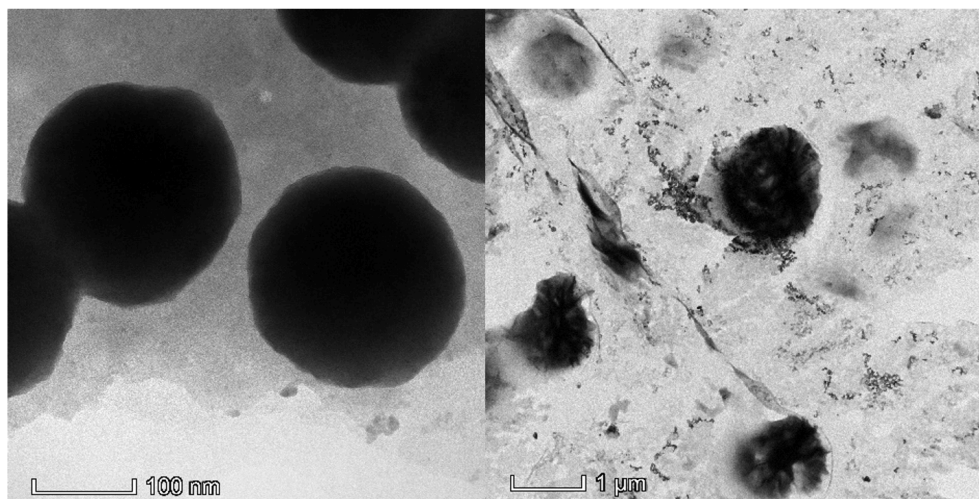


Fig. 8. Exosome sample shows that it changes in terms of morphology and numbers of vesicles surrounds the cell after being exposed to SAW

In terms of the shape of the vesicles, it can be seen before and after, the vesicles are crushed and the vesicle membrane breaks. This is influenced by the acoustic pressure produced when the sample is exposed to SAW.

#### 4. Conclusions

Lysing mechanism for extracellular vesicles through cavitation technique results in cells breaking through a combination of shear forces and pressure changes without destroying proteins and nucleic acids. The Bradford test was used to observe an increase in the presence of proteins resulting from the rupture of extracellular vesicles after exposure to directed acoustic waves. Based on the test results, it can be concluded that the power of the most optimal exposure time period and SAW power are at 20dBm for 60 seconds. It can also be observed in this experiment that a too long period of exposure will generate heat which results in proteins that come out of the extracellular vesicles undergo degradation. It can be concluded that the results of this study prove that by integrating the focused SAW device and the PDMS microfluid chamber Y-flow micro mixing, biological cell analysis as well as cell lysing of biological samples can be done more effectively using SAW.

#### Acknowledgement

This research was funded by a grant from Ministry of Education Malaysia (FRGS/1/2019/TK04/UKM/02/1).

#### References

- [1] Foo, Jhi Biau, Qi Hao Looi, Chee Wun How, Sau Har Lee, Maimonah Eissa Al-Masawa, Pei Pei Chong, and Jia Xian Law. "Mesenchymal stem cell-derived exosomes and micrnas in cartilage regeneration: Biogenesis, efficacy, mirna enrichment and delivery." *Pharmaceuticals* 14, no. 11 (2021): 1093. <https://doi.org/10.3390/ph14111093>
- [2] Othman, Norahayu, Rahman Jamal, and Nadiah Abu. "Cancer-derived exosomes as effectors of key inflammation-related players." *Frontiers in immunology* 10 (2019): 2103. <https://doi.org/10.3389/fimmu.2019.02103>
- [3] Berumen Sánchez, Greg, Kaitlyn E. Bunn, Heather H. Pua, and Marjan Rafat. "Extracellular vesicles: Mediators of intercellular communication in tissue injury and disease." *Cell Communication and Signaling* 19, no. 1 (2021): 1-18. <https://doi.org/10.1186/s12964-021-00787-y>
- [4] Colombo, Marina, Graça Raposo, and Clotilde Théry. "Biogenesis, secretion, and intercellular interactions of exosomes and other extracellular vesicles." *Annual review of cell and developmental biology* 30 (2014): 255-289. <https://doi.org/10.1146/annurev-cellbio-101512-122326>
- [5] Pucci, Ferdinando, Christopher Garris, Charles P. Lai, Andita Newton, Christina Pfirschke, Camilla Engblom, David Alvarez et al. "SCS macrophages suppress melanoma by restricting tumor-derived vesicle–B cell interactions." *Science* 352, no. 6282 (2016): 242-246. <https://doi.org/10.1126/science.aaf1328>
- [6] György, Bence, Tamás G. Szabó, Mária Pásztói, Zsuzsanna Pál, Petra Misják, Borbála Aradi, Valéria László et al. "Membrane vesicles, current state-of-the-art: emerging role of extracellular vesicles." *Cellular and molecular life sciences* 68, no. 16 (2011): 2667-2688. <https://doi.org/10.1007/s00018-011-0689-3>
- [7] Jamaludin, Nur Mas Ayu, Muhammad Khairulanwar Abdul Rahim, Azrul Azlan Hamzah, Nadiah Abu, and Muhamad Ramdzan Buyong. "Optimization of the Isolation of Extracellular Vesicles via Dielectrophoresis: A preliminary Analysis." *International Journal of Nanoelectronics & Materials* 13 (2020).
- [8] JAMALUDIN, NURMASAY, Muhammad Khairulanwar Abdul Rahim, Azrul Azlan Hamzah, Nadiah Abu, and Muhamad Ramdzan Buyong. "Rapid Manipulation of Extracellular Vesicles using Dielectrophoretic Mechanism." *Sains Malaysiana* 49, no. 12 (2020): 2901-2912. <https://doi.org/10.17576/jsm-2020-4912-03>
- [9] Abu, Nadiah, and Nurul Ainaa Adilah Rus Bakaruraini. "The interweaving relationship between extracellular vesicles and T cells in cancer." *Cancer Letters* 530 (2022): 1-7. <https://doi.org/10.1016/j.canlet.2021.12.007>
- [10] Chen, Jiacy, Peilong Li, Taiyi Zhang, Zhipeng Xu, Xiaowen Huang, Ruiming Wang, and Lutao Du. "Review on strategies and technologies for exosome isolation and purification." *Frontiers in Bioengineering and Biotechnology* 9 (2022): 811971. <https://doi.org/10.3389/fbioe.2021.811971>

- [11] Zhao, Zheng, Harshani Wijerathne, Andrew K. Godwin, and Steven A. Soper. "Isolation and analysis methods of extracellular vesicles (EVs)." *Extracellular vesicles and circulating nucleic acids* 2 (2021): 80. <https://doi.org/10.20517/evcna.2021.07>
- [12] Zhang, Ning, Nianrong Sun, and Chunhui Deng. "Rapid isolation and proteome analysis of urinary exosome based on double interactions of Fe<sub>3</sub>O<sub>4</sub>@ TiO<sub>2</sub>-DNA aptamer." *Talanta* 221 (2021): 121571. <https://doi.org/10.1016/j.talanta.2020.121571>
- [13] Zhou, Y., K. Yang, J. Cui, J. Y. Ye, and C. X. Deng. "Controlled permeation of cell membrane by single bubble acoustic cavitation." *Journal of controlled release* 157, no. 1 (2012): 103-111. <https://doi.org/10.1016/j.jconrel.2011.09.068>
- [14] Shehadul Islam, Mohammed, Aditya Aryasomayajula, and Ponnambalam Ravi Selvaganapathy. "A review on macroscale and microscale cell lysis methods." *Micromachines* 8, no. 3 (2017): 83. <https://doi.org/10.3390/mi8030083>
- [15] Zhang, Hua, and Wenrui Jin. "Determination of different forms of human interferon- $\gamma$  in single natural killer cells by capillary electrophoresis with on-capillary immunoreaction and laser-induced fluorescence detection." *Electrophoresis* 25, no. 7-8 (2004): 1090-1095. <https://doi.org/10.1002/elps.200305803>
- [16] Han, Shanying, Yueshuang Xu, Jie Sun, Yufeng Liu, Yuanjin Zhao, Weiguo Tao, and Renjie Chai. "Isolation and analysis of extracellular vesicles in a Morpho butterfly wing-integrated microvortex biochip." *Biosensors and Bioelectronics* 154 (2020): 112073. <https://doi.org/10.1016/j.bios.2020.112073>
- [17] Meng, Long, Feiyan Cai, Qiaofeng Jin, Lili Niu, Chunxiang Jiang, Zhanhui Wang, Junru Wu, and Hairong Zheng. "Acoustic aligning and trapping of microbubbles in an enclosed PDMS microfluidic device." *Sensors and Actuators B: Chemical* 160, no. 1 (2011): 1599-1605. <https://doi.org/10.1016/j.snb.2011.10.015>
- [18] Shehadul Islam, Mohammed, Aditya Aryasomayajula, and Ponnambalam Ravi Selvaganapathy. "A review on macroscale and microscale cell lysis methods." *Micromachines* 8, no. 3 (2017): 83. <https://doi.org/10.3390/mi8030083>
- [19] Taller, Daniel, Katherine Richards, Zdenek Slouka, Satyajyoti Senapati, Reginald Hill, David B. Go, and Hsueh-Chia Chang. "On-chip surface acoustic wave lysis and ion-exchange nanomembrane detection of exosomal RNA for pancreatic cancer study and diagnosis." *Lab on a Chip* 15, no. 7 (2015): 1656-1666. <https://doi.org/10.1039/C5LC00036J>
- [20] Farooq, Umar, Xiufang Liu, Wei Zhou, Muhammad Hassan, Lili Niu, and Long Meng. "Cell lysis induced by nanowire collision based on acoustic streaming using surface acoustic waves." *Sensors and Actuators B: Chemical* 345 (2021): 130335. <https://doi.org/10.1016/j.snb.2021.130335>
- [21] Destgeer, Ghulam, Kyung Heon Lee, Jin Ho Jung, Anas Alazzam, and Hyung Jin Sung. "Continuous separation of particles in a PDMS microfluidic channel via travelling surface acoustic waves (TSAW)." *Lab on a Chip* 13, no. 21 (2013): 4210-4216. <https://doi.org/10.1039/c3lc50451d>
- [22] Peng, Chang, Mengyue Chen, James B. Spicer, and Xiaoning Jiang. "Acoustics at the nanoscale (nanoacoustics): A comprehensive literature review. Part II: Nanoacoustics for biomedical imaging and therapy." *Sensors and Actuators A: Physical* 332 (2021): 112925. <https://doi.org/10.1016/j.sna.2021.112925>
- [23] Li, Haiyan, James R. Friend, and Leslie Y. Yeo. "Surface acoustic wave concentration of particle and bioparticle suspensions." *Biomedical microdevices* 9, no. 5 (2007): 647-656. <https://doi.org/10.1007/s10544-007-9058-2>
- [24] Heron, Scott R., Rab Wilson, Scott A. Shaffer, David R. Goodlett, and Jonathan M. Cooper. "Surface acoustic wave nebulization of peptides as a microfluidic interface for mass spectrometry." *Analytical chemistry* 82, no. 10 (2010): 3985-3989. <https://doi.org/10.1021/ac100372c>
- [25] Lyford, T. J., P. J. Millard, and M. Pereira da Cunha. "Cell Lysis using surface acoustic wave devices for sensor applications." In *2012 IEEE International Ultrasonics Symposium*, pp. 1216-1219. IEEE, 2012. <https://doi.org/10.1109/ULTSYM.2012.0303>
- [26] Zain, Mimie Asmiera Mohd, Norazreen Abd Aziz, and Muhamad Ramdzan Buyong. "Particle separation using acoustic wave device for microfluidic applications." *Journal of Advanced Research in Fluid Mechanics and Thermal Sciences* 52, no. 1 (2018): 104-114.
- [27] Zainal, Nazihah, Norazreen Abd Aziz, Fatin Afika Abdul Mutalib, and Muhamad Ramdzan Buyong. "Chaotic mixing of microdroplets using surface acoustic waves device." *Journal of Advanced Research in Fluid Mechanics and Thermal Sciences* 73, no. 1 (2020): 13-24. <https://doi.org/10.37934/arfmts.73.1.1324>
- [28] Chen, Yuchao, Xiaoyun Ding, Sz-Chin Steven Lin, Shikuan Yang, Po-Hsun Huang, Nitesh Nama, Yanhui Zhao et al. "Tunable nanowire patterning using standing surface acoustic waves." *ACS nano* 7, no. 4 (2013): 3306-3314. <https://doi.org/10.1021/nn4000034>

- [29] Guo, Feng, Peng Li, Jarrod B. French, Zhangming Mao, Hong Zhao, Sixing Li, Nitesh Nama, James R. Fick, Stephen J. Benkovic, and Tony Jun Huang. "Controlling cell–cell interactions using surface acoustic waves." *Proceedings of the National Academy of Sciences* 112, no. 1 (2015): 43-48. <https://doi.org/10.1073/pnas.1422068112>